Title:

Large-scale explosive arena trials – is your target being loaded correctly?

Authors:

Thomas Payne BSc MSc PhD[1*], Andrew Williams CEng MICE MCIOB AIExpE[1], Thomas Worfolk BEng AMIET[1], Samuel Rigby MEng PhD MIExpE[2]

1. Introduction

Internationally, a substantial body of experimental testing has been conducted to assess the performance of glazing and other structural components, such as walls and doors, under blast loading. This often takes place in large-scale arena tests and involves setting up numerous targets at different ranges around a central charge. This setup is employed to maximise the usable arena space in each shot, thereby improving cost-efficiency and helping to achieve 'best value'.

Overall, arena test charge sizes can vary from 10s of kg to 10s of tonnes, but the most common charge sizes in UK testing are in the 100s of kg range, all measured in TNT equivalence (TNT_e).

UK arena testing of glazing commonly follows the general principles of *ISO16933:2007 Glass in Building – Explosion-resistant Security Glazing – Test and Classification for Arena Air-blast Loading*. Glazing targets are commonly 1.25 x 1.55 m in size and are typically mounted in cubicles; either 2.4 m wide x 2.4 m high front-face dimensions with a single landscape aperture, or 3.2 m wide x 3.15 m high front-face dimensions with twin portrait apertures, as shown in Figure 1.

UK arena testing of walls and doors commonly follows *21/09 Home Office Test Standard for Protected Spaces (Explosion Resistant Walls and Doors)*. Wall targets are commonly constructed up to 3.0 m wide x 3.5 m high and mounted within a cubicle formed from reinforced concrete culvert units 3.45 m wide x 3.9 m high, as shown in Figure 1

[1] Home Office Centre for Applied Science and Technology, Langhurst House, Langhurstwood Road, Horsham, West Sussex RH12 4WX

*Corresponding author.

[2] Department of Civil and Structural Engineering, University of Sheffield, Mappin Street, Sheffield S1 3JD

Figure 1 – Typical glazing targets mounted in a single aperture cubicle and a double aperture cubicle, and a typical wall target mounted in a reinforced concrete cubicle

(courtesy of DNV GL)

The actual blast loading imposed on the targets during testing is generally measured using a reinforced concrete gauge block of a similar size to the target, positioned at a matching range and with pressure transducers mounted in appropriate locations, flush with the face of the gauge block.

By assuming a hemispherical blast front, one can infer identical loadings on targets of the same size located at the same range as well as on appropriately-sized and located gauge blocks.

However, problems may occur where targets are placed too close together and blast load interactions with individual targets begin to interfere with the loading experienced by other neighbouring targets.

Aside from experimental testing, predicted loadings can also be derived using suitably validated software codes. This study uses one such code to assess the influence of target placement on the blast loading experienced.

2. Blast wave interaction

When a blast wave hits a target of finite size, it reflects from it and diffracts around it, modifying the pressure-time histories of nearby waves. Reflections can result in an amplification effect through a superposition with the incident blast wave (see Figure 2a). Diffractions can result in a shielding (or shadowing) effect decreasing the intensity of the blast wave, such as in the region behind the structure (Remennikov and Rose, 2005; Needham, 2009) (see Figure 2b).

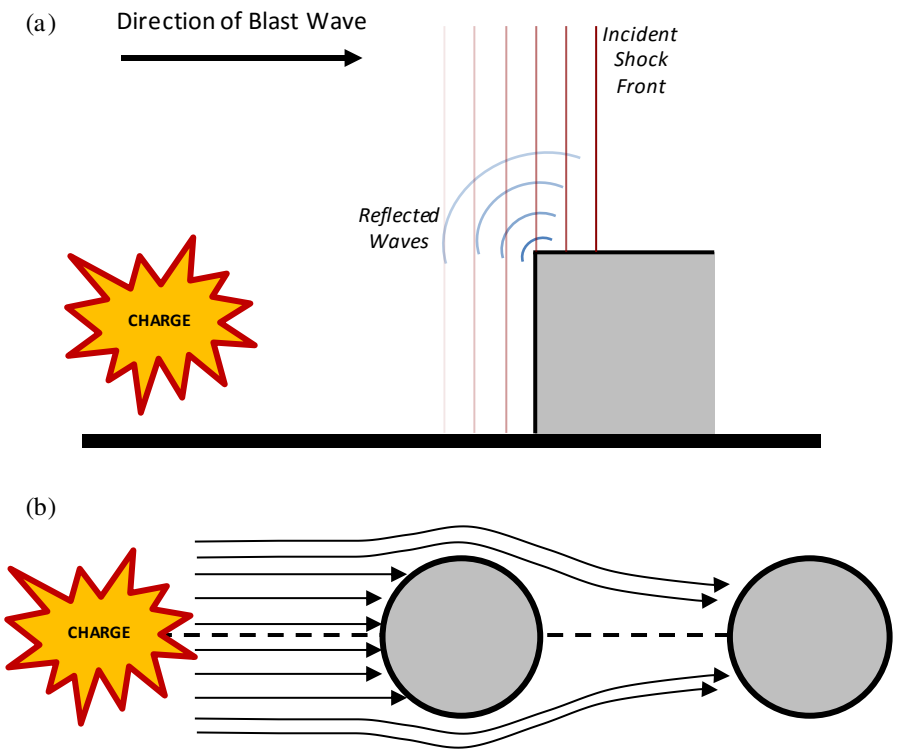

Figure 2 – Schematic showing formation of: (a) an amplification effect and (b) a shielding effect.

Previous research investigating the interactions of blast waves with structures has focused largely on the local 'clearing' effects experienced by structures of finite size when exposed to a blast wave (Rickman and Murrell, 2007; Shi *et al.*, 2007; Ballantyne *et al.*, 2009; Qasrawi *et al.*, 2015). Recent studies have led to new perspectives on the mechanisms for the clearing effect and proposed methods to calculate their extent (Rigby *et al.*, 2014a).

In terms of blast wave interference, a growing body of research has been conducted investigating blast loadings in urban streetscape environments. Early work conducted by Smith and Rose (2000) investigated the features of urban streetscape environments that amplify blast effects using experimental study and computational fluid dynamics (CFD) software. Remennikov and Rose (2005) subsequently conducted a detailed series of numerical simulations using Air3D CFD software to investigate shadowing and amplification effects from buildings in an urban terrain. In recent years, a significant focus has been placed upon internal explosions and different building geometries.

However, to the authors' knowledge, there are no research studies investigating the specific interferences introduced due to the proximity of neighbouring structures in arena blast trials.

Pressure and impulse are widely acknowledged to be the two key contributory factors relating to blast load damage on structures. Although the negative phase has been shown to be influential in blast damage, particularly in more frangible structures

(Rigby et al., 2014b), this study focuses on rigid targets and these effects have been neglected.

To achieve ‘best value’ in testing it is beneficial to include as many targets as possible within each arena. In practice, two engineering ‘rules of thumb’ are typically used as a guideline for engineers in the field to ensure that individual targets do not adversely influence the blast loading on other adjacent or nearby targets.

- *For two cubicle targets at the same stand-off range:* a minimum separation of two cubicle widths between the targets.
- *For two cubicle targets at different stand-off ranges*: a minimum angle of 45° between the centreline of the targets measured from the detonation point.

Examination of the interference effects of the positive phase loading phenomena from rigid target obstructions will enable more informed cubicle placement in arena blast trials. Such information could also be used to confirm the veracity of these engineering rules of thumb and potentially permit a greater number of cubicle targets to be positioned around a charge, thus increasing efficiency and reducing costs.

The following two photographs show a typical arena test setup before (Figure 3) and during (Figure 4) a test.

Figure 3 – General view of a typical arena test setup (courtesy of DNV GL)

Figure 4 – General view of a typical arena test in progress (courtesy of DNV GL)

This study aims to use conventional numerical modelling techniques to examine the influence of cubicle positioning in large-scale arena blast trials and present a series of recommendations for placement in a format that can easily be used by engineers in the field.

3. Methodology

3.1. Modelling software and approach

CFD software package Air3D (Cranfield University, UK) (Rose, 2006) was used for all simulations in this study as the software provided a verified level of blast wave fidelity and phenomenology whilst possessing a relatively low computational expenditure.

The software requires the following assumptions for any scenario:

- the ground surface and targets are considered perfectly rigid;
- the impacts of thermal shocking and detonation products are ignored;
- air and other gaseous products are treated as ideal; and
- the blast wave is assumed to be spherical/hemispherical.

To determine the influence of arena test cubicles on nearby blast waves, a series of paired simulations were run: one free-field and the other with a single obstructing cubicle target present. The differences in incident overpressure-time histories were then examined between free-field and obstructed-field simulations to identify the degree of interference in peak incident overpressure (Ps^+) and incident positive phase impulse (Is^+) from each test configuration.

In each simulation:

- The target cubicle (in obstructed-field simulations only) was fixed at a range of between 15 and 50 m in 5 m intervals.
- The cubicle was given dimensions of 3.50 m x 3.95 m x 3.00 m (width x height x depth), representative of a typical wall target.
- Arrays of pressure gauges were distributed radially in an arc from the explosive source, each array contained a total of 400 gauges evenly distributed over the region of interest at a height of 2.00 m (approximately half the cubicle height).
- The gauge arcs were positioned in 5 m stand-off intervals from the target (i.e. a 35 m stand-off target would have gauges on arcs at 35 m, 40 m, 45 m and 50 m stand-off ranges).
- A 100 kg TNTe charge (using Air3D default TNT charge parameters) was used.

An example 2D schematic of the test configuration has been shown in Figure 5.

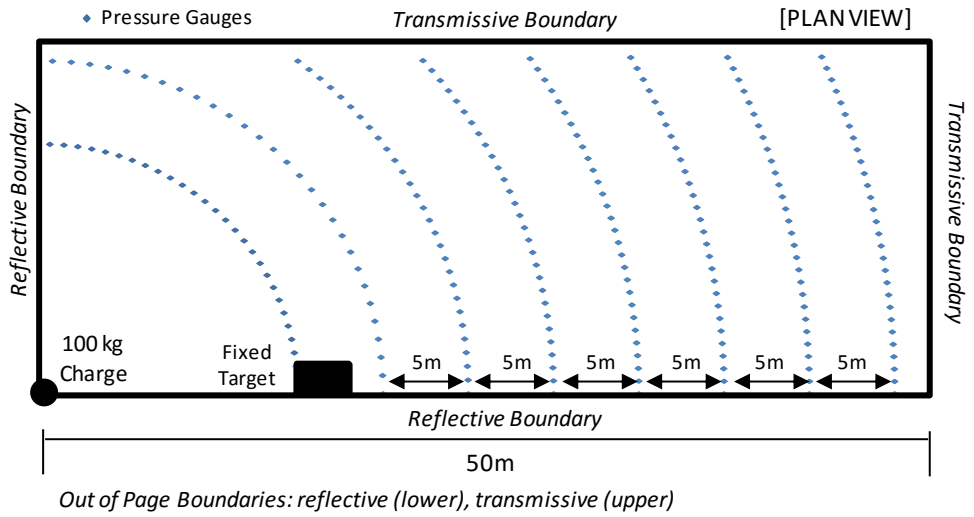

Figure 5 – Schematic of simulation test configuration

3.2. Model development and software validation

In Air3D, explosive simulations are treated in a multi-stage process through 1D, 2D and 3D domains. In the 1D domain, the simulation is performed to model the formation of the wave up to the nearest surface, in this case the ground. As it reaches this first surface it ceases to be spherically symmetric. The solution is remapped into 2D with a reflective ground surface and an axisymmetric simulation is run that models blast wave formation and propagation up to the point where it interacts with the second surface, in this case the target structure. Once it reaches this second surface it is no longer axisymmetric and the solution is remapped to a 3D

domain, where the interaction between the blast wave and the structural target is simulated.

The Air3D version 9.0 users' guide (Rose, 2006) states that "Problems should be set up initially using a discretisation that allows an accurate description of the problem geometry and captures all major aspects of the flow-field: correct number and duration of shock waves". Mesh refinements were therefore conducted in all domains to ensure that blast phenomena were adequately represented, balancing accuracy and computational cost.

A series of iterative mesh refinement simulations informed the use of 1 mm and 20 mm cell sizes for 1D and 2D simulations respectively. 3D mesh refinement simulations were compared with CONWEP (US Army Corps of Engineers, Engineer Research and Development Centre) hemispherical burst parameters to provide a measure of the absolute accuracy of the predictions (Figure 6).

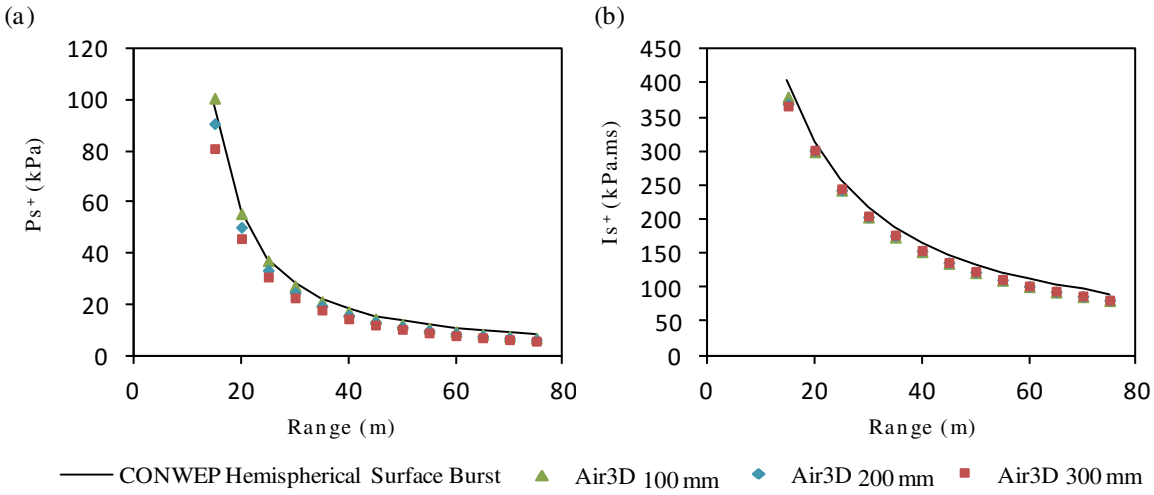

Figure 6 – Comparison of Ps^+ and Is^+ of different cell size simulations against CONWEP hemispherical burst predictions

This convergence study demonstrated a 3D cell size of 100 mm delivered a reasonable level of accuracy relative to computational costs.

The Air3D software output was further validated by conducting separate, blind predictions of a set of experimental blast trials conducted at the University of Sheffield (Tyas *et al.*, 2011). The experiments investigated clearing effects using a 250 g C4 hemispherical explosive charge against a 675 x 710 mm rigid target at ranges of 4-10 m.

Figure 7 shows a comparison between the pressure-time histories and cumulative impulse-time histories from the experimental test data and the Air3D predictions for the gauge located centrally in the target face.

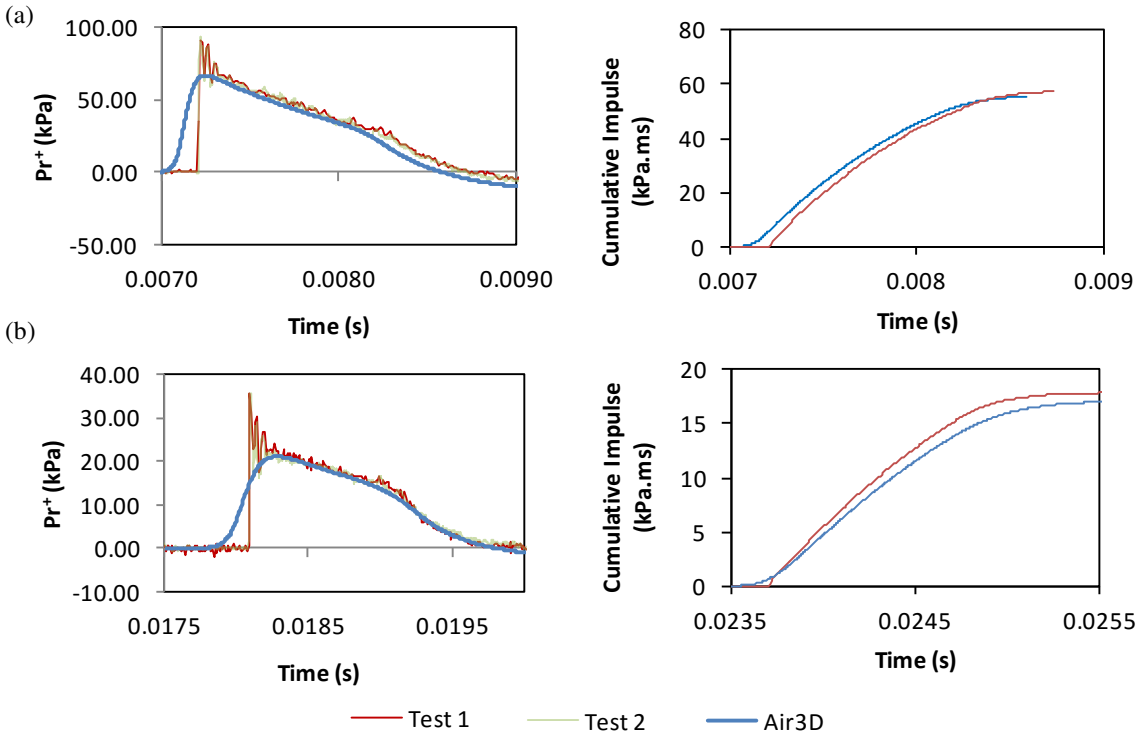

Figure 7 – Comparison between Air3D predictions and experimental test data (Tyas *et al.*, 2011) for targets at: (a) 4 m and (b) 10 m ranges

These comparisons demonstrate an acceptable level of accuracy for predicted pressure-time histories. The predictions for peak reflected, positive phase impulse (Ir^+) values were found to match the mean experimental values to within 3%.

3.3. Post-processing

Given the significant quantities of data produced by the arrays of pressure gauges, MATLAB® (Mathworks Ltd., MA, USA) was selected as the post-processing tool due to its robust and efficient processing capabilities.

In each simulation, the pressure-time histories extracted from Air3D were imported into MATLAB® and processed to determine Ps^+ and Is^+ values. The array of Ps^+ and Is^+ values from the free-field simulations were then processed alongside the corresponding values from the obstructed-field simulations to calculate the percentage difference (or interference) at each gauge position. Given an array of percentage difference values for Ps^+ and Is^+, a threshold value could be applied and the corresponding Cartesian co-ordinate location could be identified.

For instances where the fixed target and measurement location were at the same stand-off range from the charge, the straight line distance between the edge of the fixed target and the threshold co-ordinate was determined using simple Pythagoras (Figure 8a). For instances where the fixed target was at a different range to the measurement location, the straight line separation from the fixed target at the same

range was calculated. To achieve this, the equation of the line from the threshold point to the origin was calculated and used to determine the intersection with the fixed target gauge arc (Figure 8b). This point was then, in turn, used to calculate the straight line distance to the fixed target edge and the corresponding value of θ.

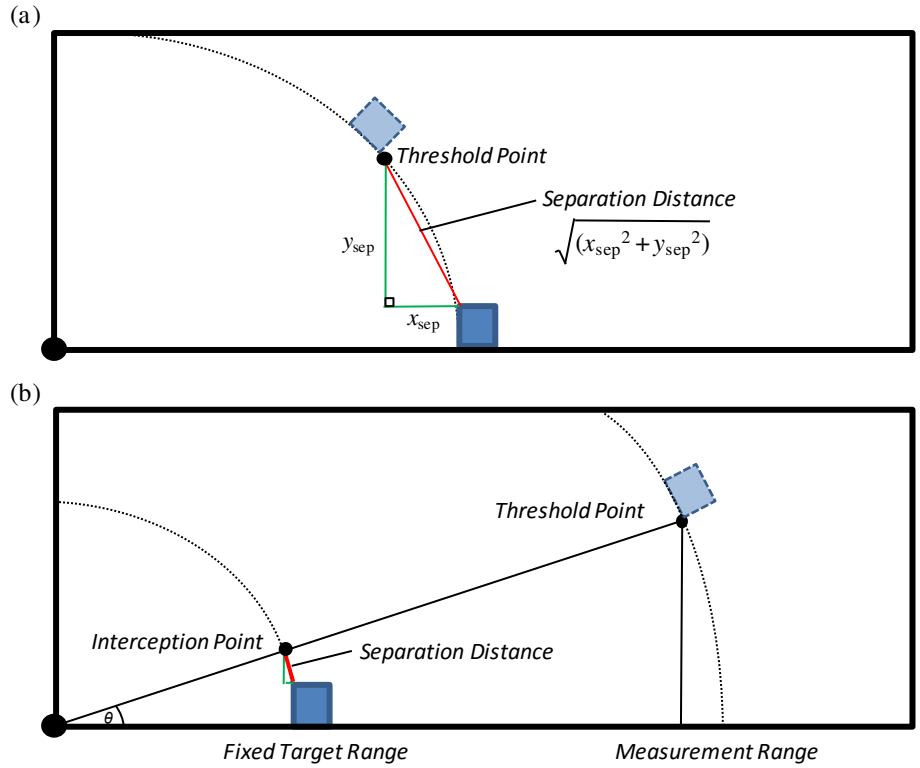

Figure 8 – Schematic showing the calculations performed to determine minimum separation distances at different interference thresholds when the fixed target and measurement positions are at: (a) the same stand-off range; and (b) different stand-off ranges

4. Results

4.1. General trends

The visualisations in Figure 9 show, in plan view, an example of peak incident overpressure (Ps^+) and incident positive phase impulse (Is^+) interference fields around a fixed target cubicle positioned at a 15 m stand-off range recorded at approximately 2 m above ground level.

Figure 9a and Figure 9c show plan views (in half symmetry) of the Ps^+ and Is^+ interference fields respectively around a fixed target cubicle positioned at a 15 m stand-off range.

Figure 9b and Figure 9d show the calculated percentage difference between the interference fields above and the associated free-field measurements expected within the domain, for Ps^+ and Is^+ respectively.

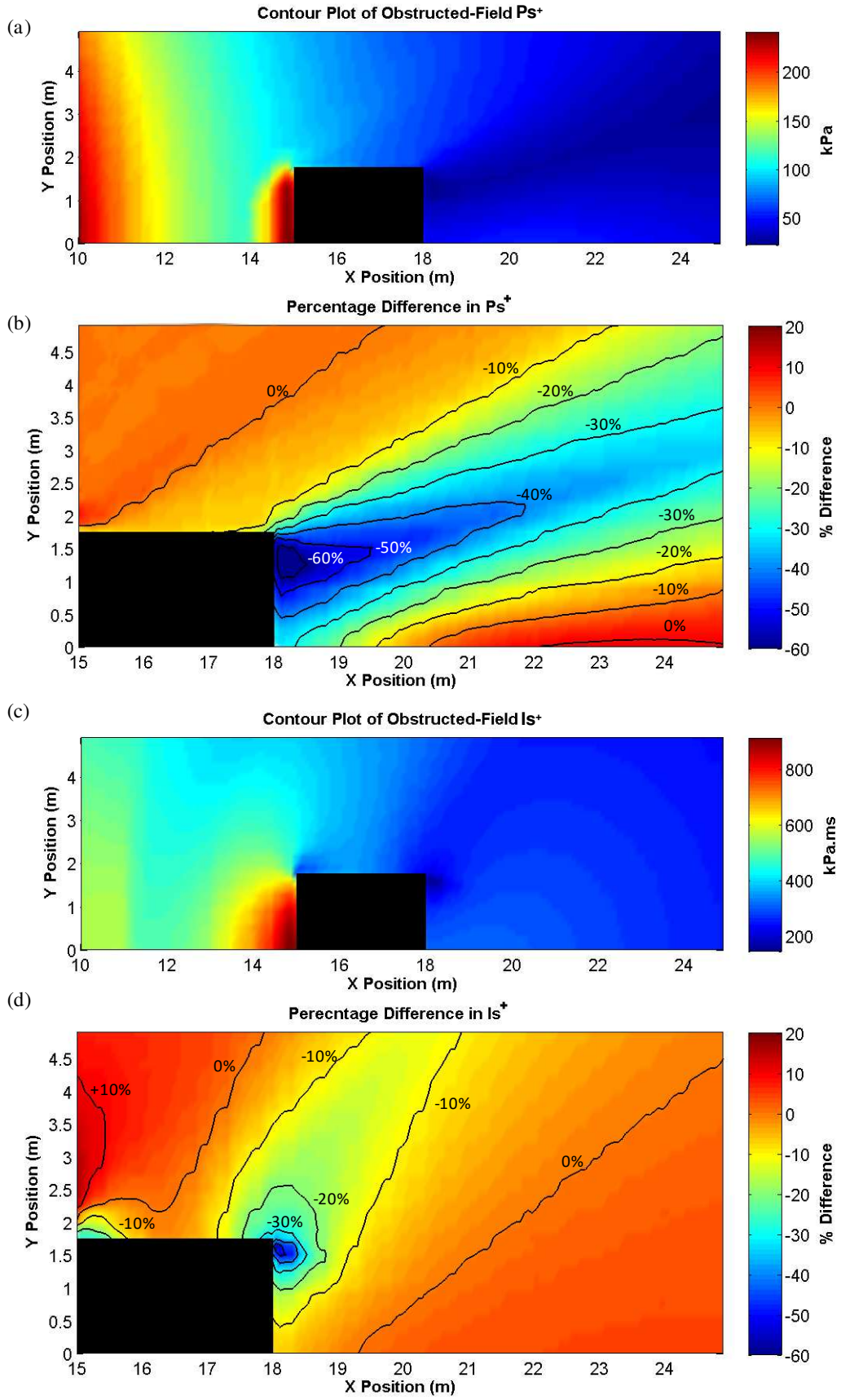

Figure 9 – Visualisations of interference by a fixed target obstacle at 15 m. Contour plots show examples of: (a) obstructed-field Ps^+; (b) percentage differences in Ps^+; (c) obstructed-field Is^+; and (d) percentage difference in Is^+

It is evident that there are differences in the magnitudes of effects of Ps^+ and Is^+ and the regions affected by the target. It is also clear that there are significantly greater differences in Ps^+ than Is^+ in the immediate proximity to the fixed target.

Figure 10 shows the radial distances from the fixed target to the position of maximum interference and limit of interference (free-field equivalent position) for Ps^+ and Is^+. In all cases, the maximum interference and the limit of interference in Ps^+ occurs at much closer proximity to the target than Is^+.

Assuming the relationship to be linear, the critical angles for maximum interference and limit of interference were 21.7° and 35.7° in Ps^+ respectively, and, 39.7° and 44.6° in Is^+ respectively. From these values, the angle for 'limit of interference' in Is^+ appears to correspond well with the 45° recommended in established rules of thumb.

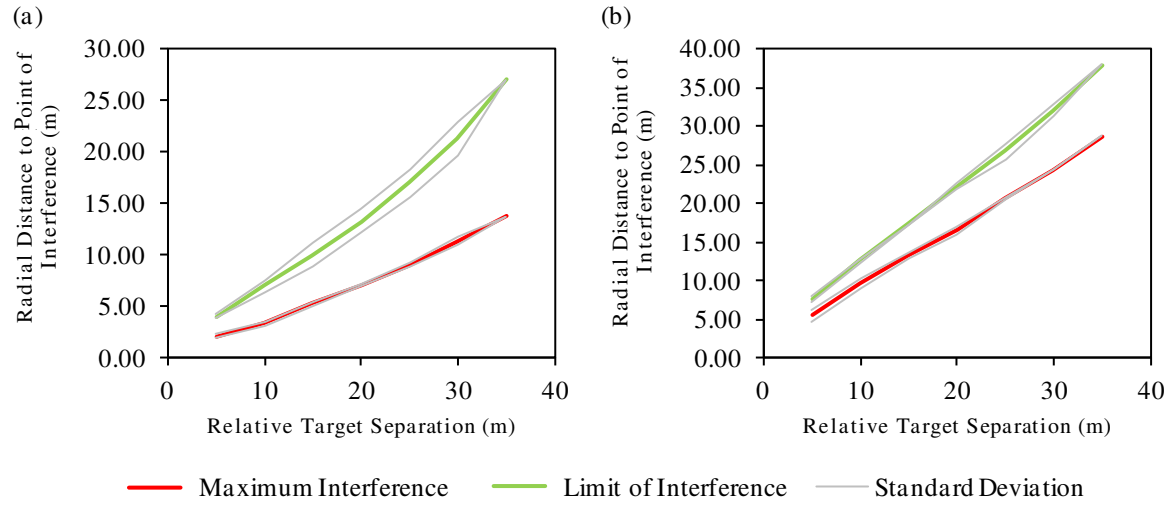

Figure 10 – Graphs showing the levels of interference introduced by fixed target obstacles at different relative target separations for: (a) Ps^+; and (b) Is^+

4.2. Recommended separation distances

As greater separation distances were required to elicit free-field equivalent Is^+ values than Ps^+ values, impulse predictions have been used to derive a series of recommended separation distances for cubicle targets in blast testing arenas. Note that the values in this table represent the separation distances required at the same range as the fixed target and, where necessary, should be used to infer target position at greater stand-off distances via the method shown in Figure 8b as the angle of the 'limit of interference' has been shown to be effectively constant with increasing distance from the explosive origin as in Figure 10.

Table 1 presents the recommended separation distances to achieve '0% threshold', or free-field equivalent Ps^+ and Is^+ values for targets at a stand-off range between 15 and 50 m. It also gives the recommended separation distance to achieve '2% Threshold' and '5% Threshold' values.

The terms ‘fixed target location’ and ‘variable target location’ in this table pertain to the method by which cubicles should be positioned. The fixed target is considered stationary with the variable target positioned relative to it.

Table 1 – Recommended clear separation distances to achieve representative (0% interference) free-field Ps^+ and Is^+ values, 2% interference values and 5% interference values for fixed and variable targets at different stand-off ranges

0% Threshold (Recommended Separation Distances)

Variable Target Location / Fixed Target Location	15 m	20 m	25 m	30 m	35 m	40 m	45 m	50 m
15 m	3.88	3.30	5.55	6.88	7.96	8.70	9.21	9.64
20 m		4.58	4.03	6.49	8.08	9.50	10.1	10.7
25 m			5.03	4.51	7.18	8.97	10.5	10.9
30 m				5.26	4.72	7.87	9.87	11.2
35 m					5.58	5.42	8.32	10.3
40 m						5.99	5.48	12.1
45 m							6.87	5.83
50 m								6.92

2% Threshold (Recommended Separation Distances)

Variable Target Location / Fixed Target Location	15 m	20 m	25 m	30 m	35 m	40 m	45 m	50 m
15 m	3.69	3.01	5.03	6.17	7.05	7.64	8.11	8.51
20 m		4.23	3.43	5.77	7.15	8.38	8.87	9.46
25 m			4.59	3.90	6.39	7.94	9.24	9.46
30 m				5.03	4.20	6.89	8.68	9.72
35 m					5.48	4.49	7.28	9.02
40 m						5.57	4.78	7.57
45 m							5.70	5.03
50 m								6.02

5% Threshold (Recommended Separation Distances)

Fixed Target Location \ Variable Target Location	15 m	20 m	25 m	30 m	35 m	40 m	45 m	50 m
15 m	3.20	2.53	4.32	5.36	6.02	6.50	6.87	7.16
20 m		3.58	2.93	4.93	6.02	7.20		
25 m			3.90	3.28	5.34	6.52	7.69	
30 m				4.05	3.53	5.62	7.27	
35 m					4.20	3.79		
40 m						4.48	3.88	
45 m							4.69	4.01
50 m								4.78

Recommended separation distance tables can be established for any given percentage interference value through further processing of the existing results dataset.

Note that in some instances, at greater interference thresholds, separation distances have not been quoted. This is because, for that specific location, the obstructed-field Is^+ value does not deviate from the free-field value by more than the relevant percentage threshold.

5. Discussion

This study provided a series of recommendations for cubicle positioning in arena blast trials through the determination of the differences in free-field pressure-time histories, with and without an obstructing target present, using numerical modelling techniques. In all conditions, there was a greater interference to peak incident overpressure (Ps^+) values than to incident positive phase impulse (Is^+) values in the region immediately surrounding the fixed target. However, Ps^+ values were found to return to free-field equivalents relatively close to the target, whilst Is^+ values remained significant at greater distances. Consequently, Is^+ interferences governed the separation distance recommendations.

To examine the appropriateness of the existing engineering rules of thumb typically used as a guideline for engineers in the field, a direct comparison has been made with the new recommendations.

In these existing rules of thumb, for targets at the same range and assuming a wall target of 3.50 m width, a practical recommendation of 7 m is given (two cubicle widths). The recommendations from the present study vary between 3.88 m and 6.92 m based on target range. This suggests that the rule of thumb is of a similar magnitude to predictions in far-field conditions, but conservative for targets in the near field where a smaller separation could be applied and more targets could potentially be distributed around the charge.

The minimum separation angle of 45° corresponds very well with the angle for the limit of Is^{+} interference of 44.6° established in this study. However, it should be noted that these measures are not directly comparable and the angles illustrated in Figure 10 have been based on an average taken from many simulations with different fixed target ranges and measurement positions (but the same relative separation). Therefore, it is likely that there will be variations based on individual test configurations. Although 45° acts as a reasonable estimate, there will be many situations where this rule of thumb will not be appropriate and the table recommendation distances should take precedence over the established rules of thumb.

6. Conclusions

In arena blast tests, a lack of careful consideration of the positioning of target cubicles around a charge can result in either: sparsely distributed targets, which poorly utilise test range space; or targets positioned too closely together, which can result in undesirable interference effects by either increasing or decreasing incident blast wave parameters.

An extensive and systematic modelling study was undertaken using Air3D to identify the differences in peak incident overpressure and incident positive phase impulse caused by a fixed target obstruction. The study indicated that, in all conditions, a greater separation distance was required to achieve free-field impulse values than free-field pressure. A bespoke series of recommendation tables has been presented for different permissible interference thresholds, which can be used by engineers in the field to identify minimum separation distances for targets at different ranges.

The results indicate that the established ‘rules of thumb’ for separation of targets at different ranges (45°) still hold some practical relevance, whilst the recommendation for targets at the same range (two cubicle widths) are generally conservative and not applicable to all test configurations.

7. Acknowledgements

The analysis on which this paper is based was conducted by the Home Office Centre for Applied Science and Technology (CAST) as part of a programme of research and

development funded and directed by the Centre for the Protection of National Infrastructure (CPNI).

The authors would also like to acknowledge the University of Sheffield for the experimental test data provided for validation.

All photographs in this paper were taken at DNV GL Spadeadam Testing and Research located at RAF Spadeadam in Cumbria.

8. References

Ballantyne, G. J., Whittaker, A. S., Dargush, G. F. and Aref, A. J. (2009) 'Air-blast effects on structural shapes of finite width', *Journal of Structural Engineering*, 136 (2), pp 152–159.

Needham, C. E. (2009) 'Blast loads and propagation around and over a building', *26th International Symposium on Shock Waves,* Volume 2, pp 1359–1364. Springer Berlin Heidelberg.

Home Office Science (2010) 'Test Standard for Protected Spaces (Explosion Resistant Walls and Doors)', Home Office Scientific Development Branch, Publication No. 21/09

ISO 16933:2007(E) (2007) 'Glass in Building – Explosion-resistant Security Glazing – Test and Classification for Arena Air-blast Loading', International Organisation for Standardisation, Geneva, Switzerland

Qasrawi, Y., Heffernan, P. J. and Fam, A. (2015) 'Numerical Determination of Equivalent Reflected Blast Parameters Acting on Circular Cross Sections', *International Journal of Protective Structures*, 6 (1), pp 1–22.

Remennikov, A. M. and Rose, T. A. (2005) 'Modelling blast loads on buildings in complex city geometries', *Computers and Structures*, 83 (27), pp 2197–2205.

Rickman, D. D. and Murrell, D. W. (2007) 'Development of an improved methodology for predicting airblast pressure relief on a directly loaded wall', *Journal of Pressure Vessel Technology*, 129 (1), pp 195–204.

Rigby, S., Tyas, A., Bennett, T., Fay, S., Clarke, S. and Warren, J. (2014a) 'A numerical investigation of blast loading and clearing on small targets', *International Journal of Protective Structures*, 5 (3), pp 253–274.

Rigby, S., Tyas, A., Bennett, T., Clarke, S. and Fay, S. (2014b) 'The negative phase of the blast load', *International Journal of Protective Structures*, 5 (1), pp 1–20.

Rose, T. A. (2006) 'A Computational Tool for Airblast Calculations', *Air3d version 9 users' guide*. UK: Cranfield University.

Shi, Y., Hao, H. and Li, Z. X. (2007) 'Numerical simulation of blast wave interaction with structure columns', *Shock Waves*, 17 (1–2), pp 113–133.

Smith, P. D. and Rose, T. A. (2000) 'The influence of urban geometry on blast wave resultants', *Proceedings of the 16th Military Aspects of Blast and Shock Symposium*, vol. 10, p. 15. UK: Oxford.

Tyas, A., Warren, J. A., Bennett, T. and Fay, S. (2011) 'Prediction of clearing effects in far-field blast loading of finite targets', *Shock Waves*, 21 (2), pp 111–119.